Effects of hygrothermal, UV and SO_2 accelerated ageing on the durability of ETICS in urban environments

João L. Parracha[1,2*], Giovanni Borsoi[2], Rosário Veiga[1], Inês Flores-Colen[2], Lina Nunes[1,3], Ana R. Garcia[4,5], Laura M. Ilharco[4], Amélia Dionísio[6], Paulina Faria[2,7]

[1]LNEC, National Laboratory for Civil Engineering, Av. do Brasil, 101, 1700-066, Lisbon, Portugal

[2]CERIS, DECivil, Instituto Superior Técnico, University of Lisbon, Av. Rovisco Pais, 1049-001, Lisbon, Portugal

[3]cE3c, Centre for Ecology, Evolution and Environmental Changes, Azorean Biodiversity Group, University of Azores, 9700-042, Angra do Heroísmo, Azores, Portugal

[4]IBB – Institute for Bioengineering and Biosciences, Instituto Superior Técnico, University of Lisbon, Av. Rovisco Pais 1, 1049-001 Lisbon, Portugal

[5] Departamento de Química e Farmácia, FCT, Universidade do Algarve, Campus de Gambelas, 8005-139 Faro, Portugal

[6]CERENA, DECivil, Instituto Superior Técnico, University of Lisbon, Av. Rovisco Pais, 1049-001, Lisbon, Portugal

[7]DECivil, NOVA School of Science and Technology, NOVA University of Lisbon, 2829-516, Caparica, Portugal

*Corresponding author at: jparracha@lnec.pt (J.L. Parracha)

ABSTRACT

External Thermal Insulation Composite Systems (ETICS) have been extensively used for either new constructions or building facades retrofitting in the last decades. These systems can provide improved thermal performance to the building envelope. However, their long-term durability remains a pervasive concern, with some systems presenting relevant anomalies after few years from their application. The durability assessment of ETICS is defined by the EAD 040083-00-0404 guideline, which stated an accelerated ageing procedure based on the hygrothermal and freeze-thaw behaviour. Nevertheless, further important environmental urban conditions, such as UV radiation and atmospheric pollutants, as well as bio-susceptibility, are not envisaged in the guideline. This paper presents the results of an experimental campaign with the aim of evaluating the durability of the rendering system of several commercially available ETICS exposed to an innovative accelerated ageing procedure, which consists of hygrothermal cycles, UV radiation and air pollutants (SO_2) exposure. Physical and chemical-morphological tests were carried out prior and after each ageing cycle in order to evaluate the durability of ETICS. Biological susceptibility to moulds was also assessed. The experimental results showed that both surface hardness and surface gloss decreased after the combined effect

of the hygrothermal, UV, and SO_2 ageing cycles, whereas an increase of surface roughness was observed. Substantial colour change for all systems after the ageing procedure was observed, confirming aesthetic alteration. Traces of biological growth were detected on the systems after ageing and the contact angle decreased after the hygrothermal cycles, indicating a lower surface hydrophobicity of the systems.

Keywords: ETICS; Durability; Artificial ageing procedure; Surface properties; Mould susceptibility; Surface wettability.

Nomenclature	
a*	Red/green coordinate, according to CIELAB colour space
b*	Yellow/blue coordinate, according to CIELAB colour space
BC	Base coat
C^*_{ab}	Chroma or colour saturation
DA	Durability assessment
EPS	Expanded polystyrene
ETICS	External Thermal Insulation Composite System
FC	Finishing coat
HC	Hygrothermal cycles
ICB	Expanded cork agglomerate
L*	Lightness coordinate, according to CIELAB colour space
MW	Mineral wool
RH	Air relative humidity
RS	Rendering system
TI	Thermal insulation
ΔE^*_{lab}	Colour change
θ	Static contact angle
HT-t	Hygrothermal cycles (EOTA 2020)
UV-t	Ultraviolet radiation exposure
SO_2-t	Exposure to pollutants (SO_2)

1. Introduction

The building sector accounts for a significant portion of the world global energy consumption [1] and a significant part is related to the heating and cooling of buildings [2]. For these reasons, considerable efforts have been made over the years by the European Union (EU) through the definition of several environmental policies, which aim at minimizing the energy demand of buildings [3,4]. As a result, the construction industry

has been adapting through the implementation of eco-efficient constructive solutions, which fulfil the comfort needs without affecting the durability and safety requirements.

External Thermal Insulation Composite Systems (ETICS), also referred to as External Wall Insulation (EWI, in the UK) or Exterior Insulation Finishing Systems (EIFS, in the USA), have been widely used for either new constructions or building facades retrofitting [5,6]. These composite systems provide an improved thermal resistance to the building envelope [7,8] and present several advantages in comparison with other thermal insulation solutions, such as the correction of thermal bridges, the protection of the masonry and structural elements from thermal stress and moisture, as well as relatively low installation costs [5,9]. ETICS significantly reduce energy loss and thus contribute to a reduction of the buildings environmental impact throughout their service life [10,11].

However, the constant exposure to weathering and anthropic factors leads to physical-mechanical and aesthetical anomalies and affects the long-term durability of ETICS [12]. The durability of ETICS is affected by either the material properties or in-service environmental and anthropic degradation agents, such as water action (e.g., humidity, ice, soluble salts), mechanical action (e.g., shrinkage, substrate deformation), human action (e.g., maintenance, vandalism, pollution) and biological action (e.g., fungi, bacteria, algae) [13]. In fact, decay patterns related to adherence loss among the different layers of the system [14,15], colour change [16], low impact resistance [17], biological colonization [18-20], among others, have been reported in the literature. Previous studies [9,21] showed that most failure modes for ETICS occurred when one or more environmental agents acted synergistically with water. In fact, important degradation mechanisms such as freeze/thaw, salts crystallization and biological colonization are strongly related to the presence of water [22]. Hence, the use of water-repellent finishing coats is fundamental for the protection of the ETICS to different degradation agents [23,24].

1.1. Durability assessment of ETICS

Research studies have been carried out over the years with the aim of evaluating the durability of ETICS and also proposing innovative evaluation methods (Table 1).

Table 1. Accelerated ageing methods for ETICS.

Reference of the method	Nr. of cycles (total h)	Experimental conditions of the ageing cycles				Durability assessment tests
		Heat	Rain	Cold	UV	

							(before and after ageing)
EAD 040083-00-0404 [25]	Heat-rain cycles	80 (320)	3 h at 70 ± 5 ºC (10-30 % RH)	1 h (1 L/(m^2.min) of sprayed water at 15 ± 5 ºC)	-	-	Visual inspection, bond strength and impact resistance
	Heat-cold cycles	5 (120)	8 h at 50 ± 5 ºC (≤ 30 % RH)	-	16 h at -20 ± 5 ºC	-	
	Freeze-thaw cycles	30 (720)	-	Immersion in water at 23 ± 2 ºC for 8 h	16 h at -20 ± 2 ºC	-	
NT BUILD 495 [26]		-	1 h at 23 ± 5 ºC (50 ± 10 % RH)	1 h (15 ± 2 L/(m^2.h) of sprayed water)	1 h at -20 ± 5 ºC	1 h until reaching 35 ± 5 ºC or 50 ± 5 ºC or 75 ± 5 ºC	Visual inspection. Other tests may be included
Griciute et al. [27]		16 (672)	-	7 h (1 L/(m^2.min) of sprayed water at 20 ºC)	7 h at -12 ºC	28 h to UV radiation (35-40 W/m^2) at 40 ºC	Visual inspection, capillary water absorption and bond strength
Bochen and Gil [28]		100 (225)	-	15 min of sprayed water	1 h at -20 ºC	1 h at 50 ºC	Open porosity and pore diameter
Slusarek et al. [29]		400 (900)	-	15 min of sprayed water	1 h at – 18 ºC	1 h at 50 ºC (+ 40 ºC in the air)	Open porosity, pore diameter, water vapour permeability and bond strength
Daniotti and Paolini [21]	UV cycles	25 (25)	-	-	-	1 h exposure at 35 ºC	Visual inspection, water absorption under low pressure, water vapour permeability, bond strength
	Winter cycles (rain, freeze and heat)	10 (50)	1 h at 30 ± 2 ºC (60 ± 5 % RH)	1 h (1 L/(m^2.h) of sprayed water at 5 ºC)	3 h at -20 ± 2 ºC	-	
	Summer cycles (dry heat and rain)	25 (50)	1 h at 70 ± 5 ºC (60 ± 5 % RH)	1h (1 L/(m^2.h) of sprayed water at 20 ºC)	-	-	

According to Lewry and Crewdson [30], the durability assessment could be carried out considering four different approaches: benchmark tests, usually through accelerated ageing tests; comparative tests, allowing to calibrate the method, materials, and equipment; environmental or stress tests; and field tests, either through natural exposure/ageing or in-situ monitoring. Considering the accelerated testing, most of the research studies

available in the literature for ETICS consider temperature and moisture effects (hygrothermal behaviour) and solar radiation (UV tests) [21,25-28], which strongly affected the durability of ETICS.

In Europe, the durability assessment of ETICS is defined by the EAD 040083-00-0404 guideline [25], where the hygrothermal (heat-rain and heat-cold cycles) and the freeze-thaw performance are considered. If the capillary water absorption of the sound system is lower than 0.5 kg/m^2 at 24 h, the guideline [25] refers that no further assessment through freeze-thaw cycles is needed. Nevertheless, additional environmental and urban conditions, *i.e.*, UV radiation and atmospheric pollutants, are not envisaged in the guideline. Moreover, despite referring that all the components of the systems should maintain their characteristics during the whole service life of ETICS (*i.e.*, at least 25 years under normal and frequent maintenance actions [25]), requirements and test methods for the evaluation of the biological susceptibility of ETICS are also neglected in the document [25].

Griciute et al. [27] proposed a new accelerated ageing method (Table 1) for the evaluation of the ETICS durability considering 16 hygrothermal and UV cycles simulating a 1-year exposure to the Lithuanian climate. Results showed that ETICS with silicate-based finishing coat have higher capillary water absorption than ETICS with acrylic-based finishing coat. Bochen and Gil [28] designed an accelerated ageing method consisting of hygrothermal and UV cycles (Table 1) to evaluate the changes in the microstructure of thin-layer renders applied in thermal insulating systems. Open porosity and pore structure were assessed every 100 cycles up to 400 cycles. The authors observed that changes occurred in the pore structure of the thin-layer renders after weathering. A significant increase of the open porosity of the external surface of the render was reported. Conversely, the total porosity of the internal zone of the render decreased with ageing. Slusarek et al. [29] evaluated the impact of anomalies of the thermal insulation on the durability of ETICS considering an accelerated ageing method similar to the one used by Bochen and Gil [28] (Table 1). A significant increase of the open porosity of the finishing coat was highlighted, as well as the development of some microcracks. Moreover, the finishing coat was found to be the layer with lower durability, thus affecting the durability of the whole system.

NORDTEST method NT Build 495 [26], adopted in Norway for the assessment of the durability of ETICS on walls [31], was originally designed to assess the degradation of materials and components used in the building envelope. This ageing procedure showed that most failure modes occurred due to incorrect execution details as well as inappropriate assembly of the components of the ETICS (*i.e.*, lack of compatibility between ETICS

components). Moreover, further studies confirmed that ETICS need a long-time span for complete drying after being exposed to wind-driven rain; thus, water can achieve the thermal insulation layer, reducing its in-service thermal performance [9,12]. Additionally, a slow drying process of the ETICS can also affect biological growth, which is mostly related to high levels of moisture content [18,19].

Daniotti and Paolini [21], considering the degradation mechanisms, dynamic thermal performance, and the climatic data of Milan (Italy), developed an accelerated ageing procedure for ETICS consisting of hygrothermal and UV cycles (Table 1). The authors concluded that the effects induced by different degradation agents were not easily reproduced at a lab-scale and proposed further developments, which include outdoor exposure for the comparison of results among natural and artificial ageing as well as the development of specific tests for the correct evaluation of ETICS long-term durability.

Nevertheless, this is only possible with the analysis of the main degradation mechanisms and the identification of the agents responsible for ETICS degradation. However, previous studies were mainly focused on the accelerated ageing of ETICS either through hygrothermal cycles and/or UV radiation, and no known investigations on the assessment of ETICS after the combined effect of hygrothermal cycles, UV radiation and pollutants, in order to effectively evaluate their durability, are reported in literature.

1.2. Research aims

This paper aims at assessing the durability of the rendering system of several commercially available ETICS exposed to an innovative accelerated ageing procedure, which comprises a sequence of hygrothermal cycles, UV radiation and exposure to pollutants (SO_2). All the selected ETICS are approved for the EU market in accordance with the EAD 040083-00-0404 [25] guideline, and thus can be considered with adequate performance and suitable quality. Nevertheless, the present study intended to go further on the analysis of the durability of the rendering system of the ETICS by considering the effects of different ageing cycles and determining physical and chemical-morphological properties, other than those mentioned in the guideline [25]. Those properties were defined to evaluate the variation of ETICS condition prior and after each ageing cycle. The biological susceptibility to moulds of the surface of the systems after each selected ageing cycle was also investigated. By providing an exhaustive insight on the durability of the rendering system of ETICS to a set of consecutive and complementary ageing tests, a deeper comprehension of the relation among ETICS degradation mechanisms and the synergistic effect of environmental agents is provided.

2. Materials and methods

2.1. Materials and ETICS systems

Six commercially available certified ETICS (each of them with a European Technical Approval (ETA)) were selected and tested. The ETA are assigned by an independent institute belonging to EOTA (European Organization for Technical Approval) and subjected to acceptance by all the EOTA members institutes. The ETICS (Figure 1) have different thermal insulation materials (EPS, ICB, or MW), base coat (cement or hydraulic lime-based), and finishing coat (acrylic, silicate, or lime-based). The identification and composition of the ETICS, according to the information provided by the manufacturers, are described in Table 2.

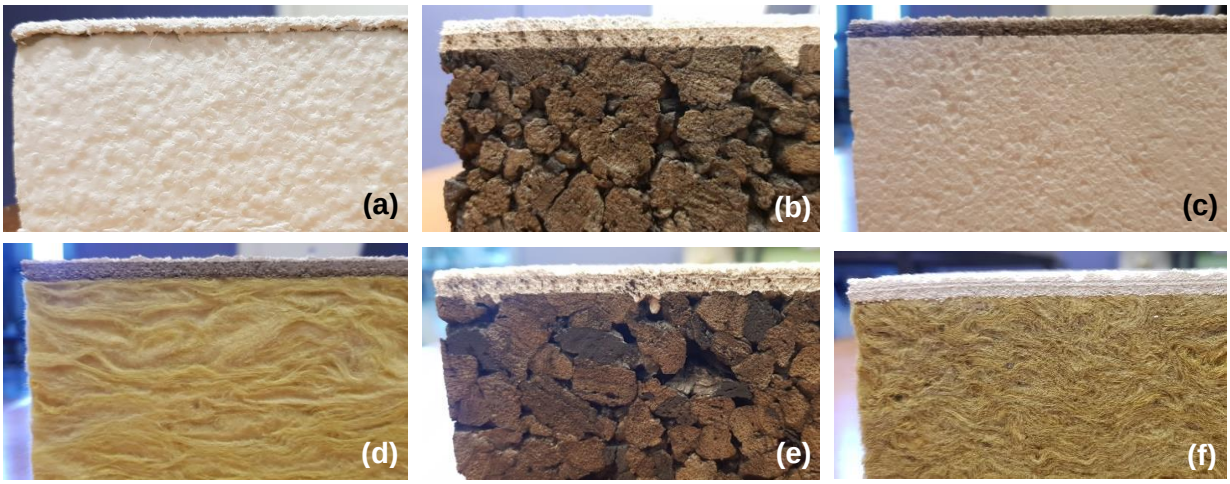

Figure 1. Photographs of E1 (a), E2 (b), E3 (c), E4 (d), E5 (e), and E6 (f).

Table 2. Identification and composition of the ETICS.

System	Thermal insulation (TI)	Rendering system (RS)		System thickness [mm]
		Base coat (BC)*	Finishing coat (FC)	
E1	EPS	Cement, synthetic resins, mineral additives	Acrylic-based, biocide**	39.87
E2	ICB	Natural hydraulic lime, cement, mineral fillers, resins and synthetic fibers	Air lime, hydraulic binder, and organic additives	65.85
E3	EPS	Cement, mineral fillers, resins and synthetic fibers	Acrylic-based, biocide**	64.53
E4	MW		Acrylic-based, biocide**	61.34
E5	ICB	Natural hydraulic lime, mixed binders, and cork aggregates	Silicate-based	43.91
E6	MW	Cement, natural hydraulic lime, and aggregates	Acrylic-based, siloxane resin, biocide**	44.77

Notation: *Includes a standard or reinforced glass fiber mesh; ** e.g., terbutryn or isothiazole

2.2. Accelerated ageing procedure

An innovative accelerated ageing procedure was defined under a research project (WGB_Shield, Figure 2). The procedure consists of hygrothermal cycles, UV radiation and air pollutant (SO_2) exposure tests. Biological susceptibility to moulds was also assessed after the hygrothermal cycles and at the end of all the selected ageing tests (Figure 2). Table 3 presents the ageing procedure designed by considering reference European standards and guidelines [25,32] and previous studies for European urban areas [33]. The procedure intends to replicate in laboratory several degradation actions that actually occur in practice and are not included in normalized or reported assessment.

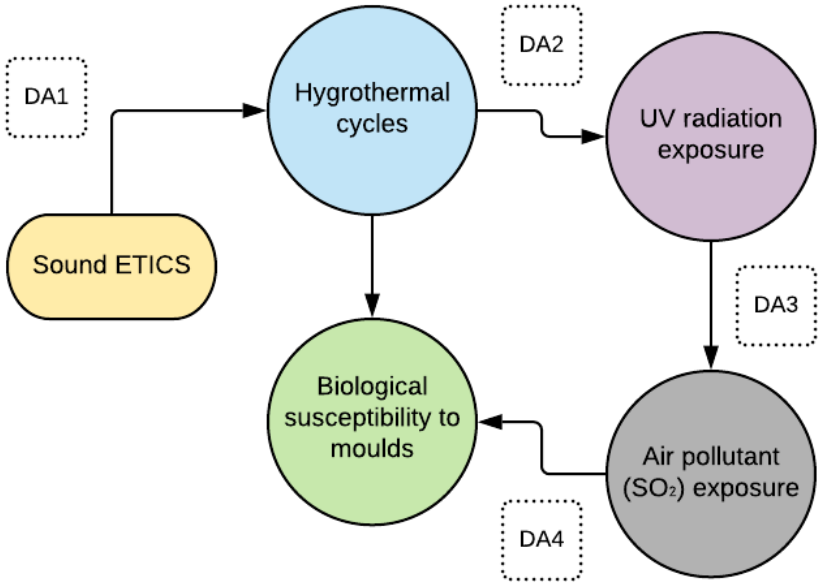

Figure 2. Scheme of the WGB_Shield accelerated ageing procedure (DA1 to DA4: Durability Assessment).

Hygrothermal cycles (Figure 2) were carried out according to EAD 040083-00-0404 [25], as resumed in Table 3, and were conducted in a FitoClima 700EDTU climatic chamber from Aralab. Two specimens of each system (S) with dimensions of 150 mm × 150 mm × System thickness (mm, Table 2) were used. The thermal insulation (TI) layer of the systems was previously protected by using metallic scotch tape and a sealing adhesive. The specimens were then vertically fixed on a rack at 50 cm from sprinklers (with a total water flux of 1 L/(m^2.min)) and thermal IR lamps (8 × 250 W). 80 repetitions of heat/rain cycles were then performed, in a total of 320 h (Table 3). Between the heat/rain and the heat/cold cycles, ETICS were left to drain for 2 h and then conditioned for 48 h at room temperature (15 ºC ≤ T ≤ 25 ºC; RH ≥ 50 %). Five repetitions of heat/cold cycles, in a total of 120 h, were performed after the heat/rain cycles.

Table 3. Details of the WGB_Shield accelerated ageing procedure for ETICS.

Method description		Nr. of cycles (total h)	Test conditions	Reference
Hygrothermal behaviour	Heat/rain cycles	80 (320)	3 h at 70 ± 5 ºC (10-30 % RH) 1 h (1 L/(m^2.min) of sprayed water at 15 ± 5 ºC	EAD 040083-00-0404 [25]
	Heat/cold cycles	5 (120)	8 h at 50 ± 5 ºC (≤ 30 % RH) 16 h at -20 ± 5 ºC	
UV exposure	UV- t/RH% cycles	125 (1000)	4 h of UV-A exposure at 60 ºC 4 h of condensation (T = 50 ºC and 80% RH)	ISO 16474-3 [32]
Exposure to pollutants	SO_2 - t/RH% cycles	60 (720)	6 h of 25 ppm SO_2 (T = 40 ºC and 30 % RH) 6 h of 25 ppm SO_2 (T = 15 ºC and 85% RH)	Gomes et al. [33]

UV radiation accelerated weathering test was carried out in accordance with ISO 16474-3 [32] and was conducted in an UV-light chamber from Q-Panel (Figure 3). Two specimens of each system resulting from the previous hygrothermal cycles (Figure 2), cut to dimensions of 100 mm × 70 mm × 20 mm, in order to match the dimension of the sample holder, were tested. During the test, the specimens were placed vertically on a rack at a distance of 10 cm from the UV source (Figure 3c). Specimens were exposed to UV-A in the range of 315 to 400 nm, and with a power of ~ 60 W/m^2 (Table 3).

(a) (b) (c) (d)

Figure 3. ETICS specimens during the hygrothermal cycles (a, b), UV weathering test (c) and air pollutant (SO_2) ageing test (d).

The influence of a highly polluted environment on the long-term durability of the ETICS was assessed by exposing the specimens to a sulphur dioxide (SO_2) rich environment using a climatic chamber FitoClima 300EDTU from Aralab (Figure 3d). Three specimens with 50 mm × 50 mm × 20 mm dimensions were cut from those used for the previous UV and hygrothermal cycles (Figure 2). The TI and BC layers of the ETICS were sealed using a metallic scotch tape and an epoxy resin, thus guaranteeing that only the FC layer was

directly exposed to the SO_2 atmosphere. Specimens were placed in the chamber for 30 days (60 cycles) (Table 3), with a concentration SO_2 of 25 ppm (diluted at 3 % in 3000 ppm of nitrogen). This value is over 30 000 times higher than the current SO_2 levels in most European urban areas [34].

Biological susceptibility to moulds was assessed following a method adapted from ASTM D5590-17 [35] and ASTM C1338-19 [36] and validated elsewhere [12]. Three specimens of each system resulting from the ageing cycles (50 mm × 50 mm × 20 mm) were tested (Figure 2). A mixed fungal suspension of *Aspergillus niger* and *Penicillium funiculosum* was prepared. The final solution was then uniformly applied (2 mL/application) on the FC of the previously steam sterilized specimens, controls, and surrounding culture media. The culture media was prepared using 4 % malt and 2 % agar concentrations. The test flasks were incubated for four weeks in a culture chamber (T = 22 ± 1 ºC and 70 ± 5 % RH) after inoculation. Three replicates of Whatman nº 1 filter paper (45 mm diameter) and three wood samples (*Pinus pinaster*) were used as controls, thus allowing the validation of the test [36]. The specimens and controls were visually rated for mould growth each week using the scale defined in ASTM D5590-17 [35]: 0 for no apparent growth (0% contaminated surface); 1 for traces of growth (< 10% contaminated surface); 2 for light growth (between 10 and 30% contaminated surface); 3 for moderate growth (between 30 and 60% contaminated surface); and 4 for heavy growth (> 60% contaminated surface). At the end of the 4-week testing, specimens and controls were carefully removed from the test flasks and the final percentage of contaminated surface was again visually rated using a stereo microscope Olympus B061.

2.3. Durability assessment

A set of tests (DA) was defined to evaluate the ETICS durability throughout the artificial ageing. These tests were performed immediately prior and after the different artificial ageing cycles, as shown in Figure 2.

Initially, ETICS surfaces were observed with the aim of detecting macroscopically visible anomalies (e.g., cracking, stains, material loss, surface irregularities). Visual observation was complemented with optical microscopy using a stereo microscope Olympus SZH10 equipped with an Olympus DP20 video camera. Microphotographs were obtained using an Olympus SC30 image acquisition system (Olympus LabSens software).

Surface hardness was evaluated using a PCE Shore A durometer according to ASTM D2240 [37]. Specimens were analysed in twelve different points along the surface using a grid.

Surface roughness was determined using an Elcometer 223 surface profile gauge, which can measure the peak-to-valley depth up to 2 mm with a resolution of 0.001 mm. Eight measurements in different points along the substrates were collected, adopting the grid used for surface hardness.

Surface gloss was evaluated using a specular gloss meter Rhopoint Novo-Gloss Lite, by considering a 60º measurement geometry. Specimens were analysed in eight different points along the surface, in accordance with hardness and roughness tests.

Colour coordinates were evaluated by measuring the CIELAB values (L^*, a^*, b^*) and using a Chroma Meter Minolta CR-410. According to CIELAB colour space [38], a^* is the red/green coordinate, varying from $+a^*$ (red) to $-a^*$ (green), b^* is the yellow/blue coordinate, varying from $+b^*$ (yellow) to $-b^*$ (blue), and L^* is the lightness coordinate, varying from 0 to 100 (from black to white, respectively). Specimens were analysed in four different points taking three consecutive measurements per point. The illuminant D_{65} at an observer angle of 2º and displaying 50 mm diameter area was adopted for the measurements, performed in specular component included mode (SCI).

Colour change (ΔE^*_{lab}) is obtained by Equation 1. This value can be calculated considering the reference colour value and the colour value obtained for each test phase. The colour differences considering the L^*, a^* and b^* coordinates were also monitored.

$$\Delta E^*_{lab} = \sqrt{(\Delta L^*)^2 + (\Delta a^*)^2 + (\Delta b^*)^2} \quad (1)$$

A threshold value of 2 CIELAB units was considered for the colour change since higher values suggest that the colour difference is detectable by an unexperienced observer [39].

The static contact angle (θ) was measured by sessile drop technique following EN 15802 [40]. This test is based in the variation of the interface free energy (area/water drop) and is carried out by dropping 4 ± 0.4 µl of water with a micropipette on the specimen. The images were obtained by a video camera (jAi CV-A50, Spain) mounted on a microscope Wild M3Z (Leica Microsystems, Germany), and analysed using MATLAB. The contact angle is measured according to Equation 2, in which h_m is the microdrop height (mm) and a_m the contact surface diameter (mm).

$$\theta = 2\arctan\frac{2h_m}{a_m} \quad (2)$$

The final value was obtained by calculating the mean value of several static contact angle measurements. Contact angle test was not carried out in systems E3, E4 and E6, due to their high surface roughness, which lead to unreliable results.

Scanning electron microscopy (SEM) analysis was carried out using a SEM Hitachi S-2400, working at an acceleration voltage of 20 kV, and coupled with an Oxford Inca X-Sight energy dispersive X-ray spectrometer. Samples were sputtered with an Au-Pd (80:20) film before analysis.

Analysis in the mid infrared with diffuse reflectance infrared Fourier transform (DRIFT) spectroscopy was carried on unaged and aged specimens. A Bruker spectrophotometer model VERTEX 70, with MCT broadband detector (spectral range 4000-500 cm^{-1}) and resolution of 4 cm^{-1}, was used. The spectra were the result of 200 accumulated single beam spectra for the sample, divided by the spectrum of KBr (FTIR grade, used as background) with the same number of accumulated scans. The spectra were transformed into Kubelka-Munk units and the baseline corrected using the OPUS software. Assuming that the total area of the components assigned to the ν*OH modes is a measure of the sample hydrophilicity and the total area of those assigned to the ν*CH modes is a measure of its lipophilicity, the ratio between the total areas of the ν*OH and ν*CH components can be interpreted as the hydrophilicity/lipophilicity balance (HLB) of the coating [41]. In order to assess this parameter, the DRIFT spectra were deconvoluted in the 3740-2360 cm^{-1} region into a sum of components described by Voigt functions, using the peak fitting module of the Origin 7.0 program. Further deconvolution was performed in the 1915-1100 cm^{-1} region, in order to gain insight on the adsorbed water and carbonatation of the coatings.

3. Results

3.1. Surface hardness and surface roughness

Results of the surface hardness show that all accelerated ageing cycles slightly affect the surface hardness of the specimens (Figure 4), with a decrease for all systems after the combination of hygrothermal cycles and UV and SO_2 exposure (DA4). The highest decrease (10.1%) was obtained for system E2 (finished with a lime-based mortar), whereas the lowest (1.2%) was obtained for system E5 (hydraulic lime-based BC and silicate-based FC). These results are in agreement with those reported by Galvão et al. [42], which obtained higher results for the silicate-based paints after natural ageing, if compared to acrylic paints. Additionally, it can be observed that systems finished with acrylic coating and MW as thermal insulation (E4 and E6) have initial

lower hardness, if compared to the other systems. In fact, a significant hardness reduction after UV and/or SO_2 weathering tests (corresponding to DA3 and DA4 stages) is observed for these systems. Interestingly, the results of surface hardness obtained for system E3 indicate that no significant differences were obtained between the different test stages considering the standard deviation (Figure 4), meaning that the surface hardness of this system was not significantly affected by the ageing procedure.

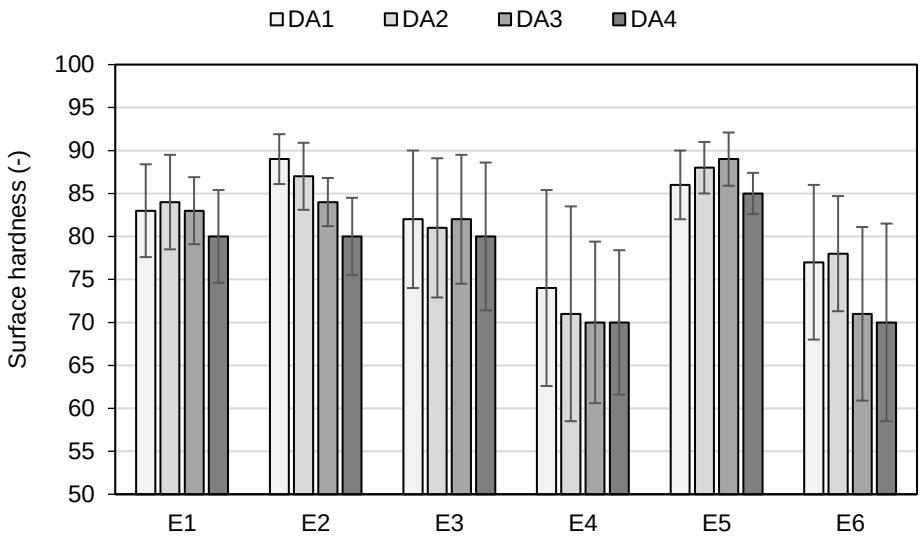

Figure 4. Surface hardness results on ETICS (average values and relative standard deviation).

Concerning surface roughness (Figure 5), systems E1 (acrylic-based FC), E2 (lime-based rendering system) and E6 (acrylic-based FC with siloxane resin) increased their surface roughness (*i.e.*, possible alteration of the surface) after the hygrothermal cycles, with the highest increase for system E2 (36.6%). Conversely, a slight decrease for systems E3 and E4 (both with acrylic-based FC) was registered after the hygrothermal cycles, with system E3 obtaining the highest decrease (16.5%). System E5 (silicate-based FC) was substantially unaffected by the hygrothermal cycles.

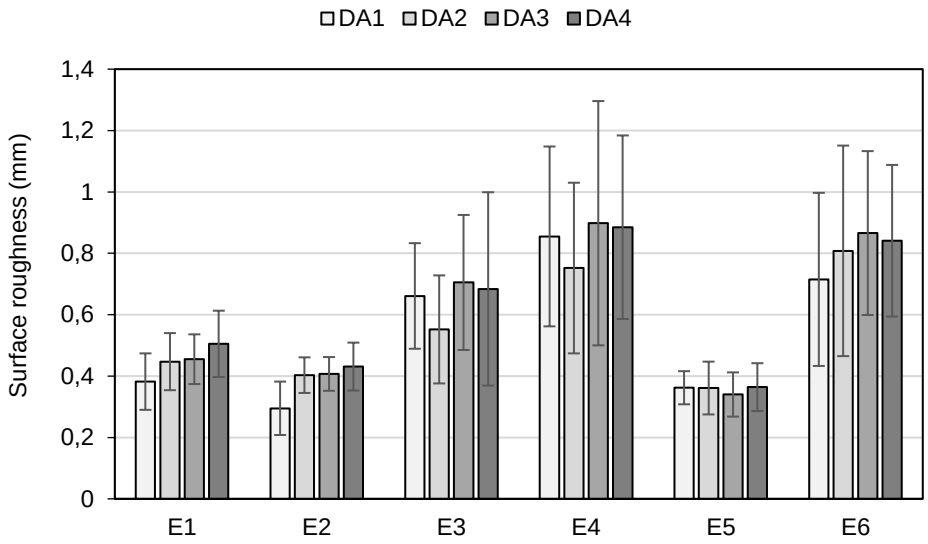

Figure 5. Surface roughness results on ETICS (average values and relative standard deviation).

After the UV ageing test most of the systems obtained higher surface roughness, if compared to hygrothermal cycles. The highest increase occurred for E3 (27.7%) and the lowest for E2 (1.0%). System E5 exhibited a slight decrease, however, its roughness is almost unaffected, if compared to the value of the sound system.

An increase of surface roughness after hygrothermal and UV cycles is also reported by other authors [43-45], ant it can be attributed to physical-chemical modifications in the coating during the cycles, with material loss from the surface as well as film shrinkage [45]. Furthermore, it is known that surface roughness can also affect the bioreceptivity, wettability and/or gloss of the coating [19,46].

Finally, the SO_2 ageing test generally induced a negligible variation of the surface roughness, when compared to the UV ageing test or the hygrothermal cycles.

It can thus be concluded that systems E1 (acrylic-based FC) (+24.4%) and E2 (lime-based rendering system) (+46.1%) presented the highest surface roughness variation after the combination of all ageing cycles, followed by system E6 (+17.6%). Systems E3 and E4, both with acrylic based FC and similar BC (Table 2), obtained significantly lower increase (in the range of +3%). The surface roughness of the system E5 (silicate-based FC) was not significantly affected by the ageing procedure (+0.55%), as no significant changes were obtained considering the standard deviation. On the other hand, the surface roughness of E2 significantly increased after the hygrothermal cycles (+36.6%), but no significant changes were observed after the UV or exposure to pollutants. The systems E3, E4 and E6 (all having acrylic-based FC) obtained the highest values of surface roughness not only in their sound state, but also after the complete ageing procedure, due to a coarser finishing

coat, when compared to the silicate-based (E5) or lime-based (E2) systems. It is interesting to note that the highest values of surface roughness obtained for E4 also led to higher values of standard deviation and a more heterogeneous surface. In fact, a rougher surface will lead to a greater dispersion of results.

3.2. Gloss and colour

Figure 6 shows the results of the specular gloss. Firstly, a slight increase of surface gloss was registered for all systems after the hygrothermal cycles (DA2), followed by a similar decrease after the UV ageing test (DA3). However, the lowest results were obtained after the combined effect of the hygrothermal cycles, UV radiation and SO_2 exposure (DA4). The highest specular gloss decrease (23.1%) was obtained for E6 (cement-based BC and a co-polymeric resin FC) and the lowest (5.0%) for E2 (finished with a lime-based mortar). Nevertheless, these results are in accordance with García and Malaga [47], who concluded that no significant gloss alteration was observed after each of the ageing cycles, as a Δgloss < 2 units is not detectable to the naked eye.

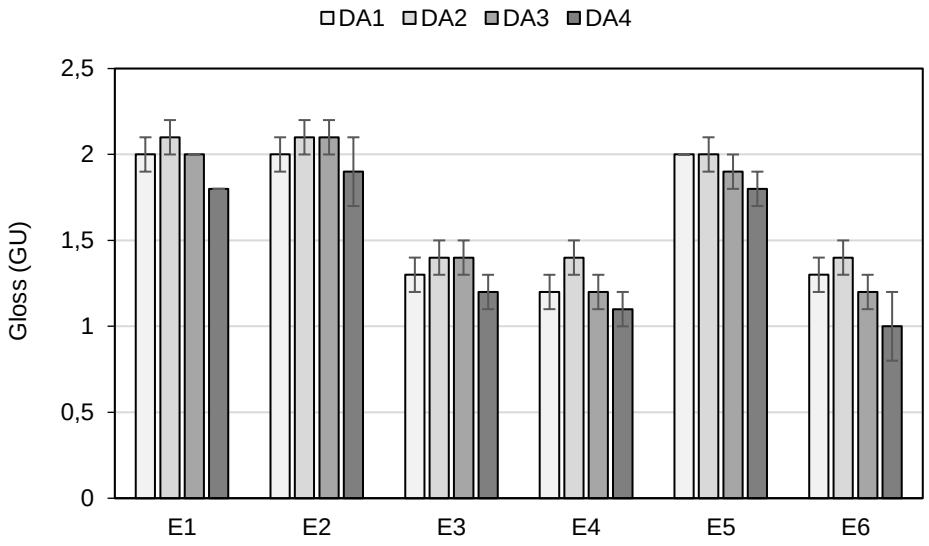

Figure 6. Specular gloss results on ETICS (average values and relative standard deviation).

When considering the colorimetric coordinates, it can be noted that lightness (L*) is strongly affected by the hygrothermal cycles (Figure 7a), with all systems presenting the highest variation (ΔL*) after these cycles (Table 4). The increase of lightness after the hygrothermal cycles is followed by a general L* decrease both after the UV (DA3) and the SO_2 ageing test (DA4) (Table 4).

Results are in agreement with those obtained by Saha et al. [48], which obtained a L* increase for acrylic polyurethane coatings exposed to an accelerated ageing test. However, after exposure to different degradation agents such as UV or SO_2, L* decreased and a trend similar to that found by Shirakawa et al. [49] is observed.

These latter authors evaluated the colour change of painted cement panels exposed in different Brazilian environments after 2 years of natural ageing and obtained a decrease of L*, an increase of b* coordinate and no significant change of a* coordinate. These observations confirm that a proper laboratorial reproduction of all the effects caused by different degradation agents, as well as valid correlation among natural and artificial ageing, is not easily achieved.

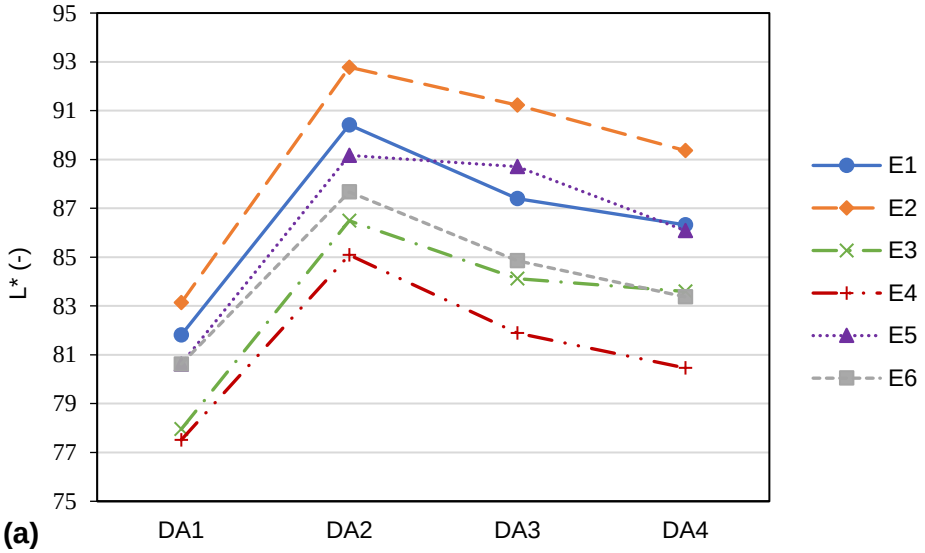

(a)

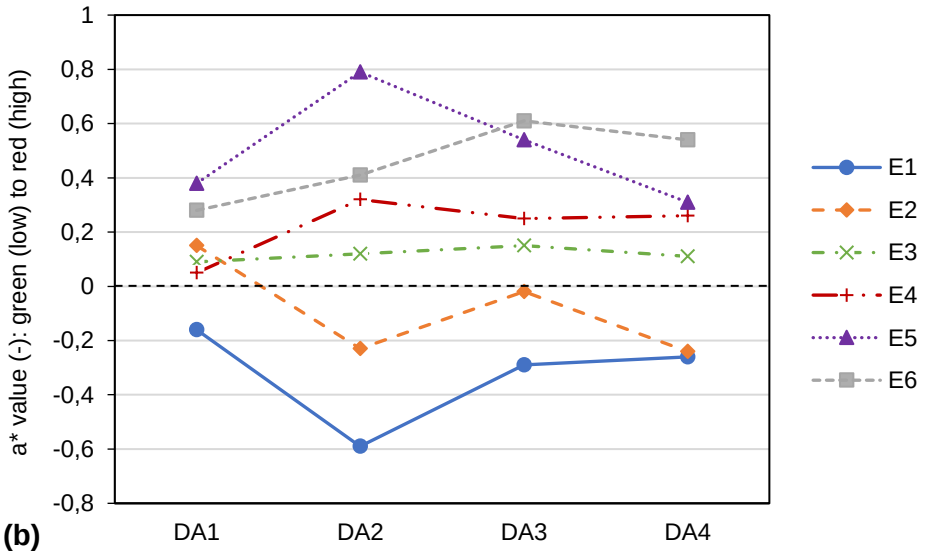

(b)

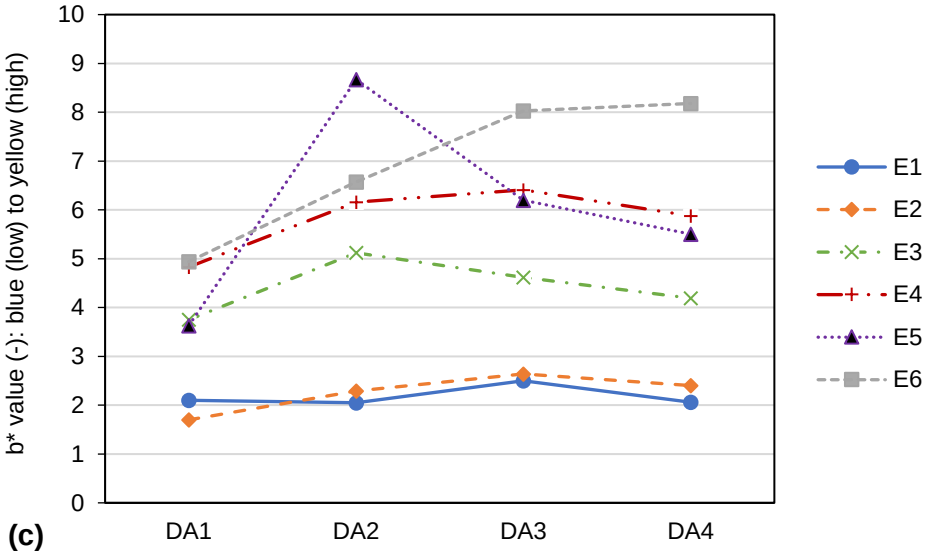

Figure 7. Variation of L* (a), a* (b) and b* (c) on ETICS throughout the WGB_Shield ageing procedure. Note: the connection between points is not a fitting result and only intends to provide a better visualization of their position throughout the ageing procedure.

System E2, with a lime-based FC, presented the highest lightness values at all test stages. In fact, E2 is among the systems that obtained lower surface roughness (Figure 5) and higher specular gloss (Figure 6). In accordance with previous studies [12,50], low values of surface roughness promote higher gloss and lightness, by increasing light reflection. Conversely, system E4 (acrylic-based FC) obtained the lowest L* values at all test stages.

Table 4. Colour variation at the end of each test phase in comparison to the colour value of unaged ETICS specimens (greyish cells: most significant variations).

	ΔL*			**Δa***			**Δb***		
	DA2	DA3	DA4	DA2	DA3	DA4	DA2	DA3	DA4
E1	8.61	5.59	4.51	-0.43	-0.13	-0.10	0.05	0.40	-0.04
E2	9.65	8.10	6.23	-0.38	-0.17	-0.39	0.59	0.94	0.70
E3	8.54	6.17	5.64	0.03	0.06	0.02	1.37	0.87	0.44
E4	7.58	4.38	2.95	0.27	0.20	0.21	1.33	1.58	1.05
E5	8.55	8.09	5.47	0.41	0.16	-0.07	5.04	2.57	1.87
E6	7.05	4.24	2.75	0.13	0.33	0.26	1.63	3.09	3.24

As observed also by visual analysis, all systems presented a yellowish to brownish coloration after the hygrothermal cycles, with an increase of the +b* values, in accordance with other authors [49,51]. The highest b* increase was obtained for E5 (silicate-based FC) and the lowest for E1 (cement-based BC and acrylic-based FC). After the UV cycles (DA3), a significant b* variation, *i.e.*, a more bluish coloration, is observed only in the case of E5. After the SO_2 exposure (DA4) most of the systems obtained lower b* values, *i.e.*, lower yellowish coloration, in comparison with those obtained after UV ageing test (DA3) (Table 4). Furthermore, at the end of the combined ageing procedure (hygrothermal + UV + SO_2), system E6 (acrylic-based and siloxane-resin FC) obtained the highest Δb (3.24), in accordance with Paolini et al. [52], which obtained a Δb of 3 CIELAB units for a white siloxane finishing coat after 3 months of natural ageing.

No significant Δa* was observed, with values close to zero (Table 4). A slight a* variation is registered only after the hygrothermal cycles, with a decrease in the case of E1 and E2 (*i.e.*, slight green component) and a slight increase for the other systems.

Regarding the global colour variation (Figure 8), the highest values, and thus major aesthetic alteration of the systems, was obtained after the hygrothermal cycles. In fact, ΔE^*_{lab} values measured for all test stages were higher than 2 CIELAB units, which means that those colour differences can be noticed by an unexperienced observer [39]. The lower ΔE^*_{lab} results after the hygrothermal + UV ageing test (DA3), when compared to those obtained after the hygrothermal test alone, can be also explained by the addition of TiO_2 on the finishing coat of the systems, as explained in more detail in Section 3.4.

Finally, a ΔE^*_{lab} decrease is observed after SO_2 exposure in the case of E1, E4 (both with acrylic-based FC), as well as E5 (silicate-based FC), whereas E2 (lime-based FC) and E3 and E6 (acrylic-based FC) show a ΔE^*_{lab} increase. In fact, the combination of SO_2 and humidity can lead to the formation of sulfuric acid, which can chemically attach the FC and induce a further colour variation [33].

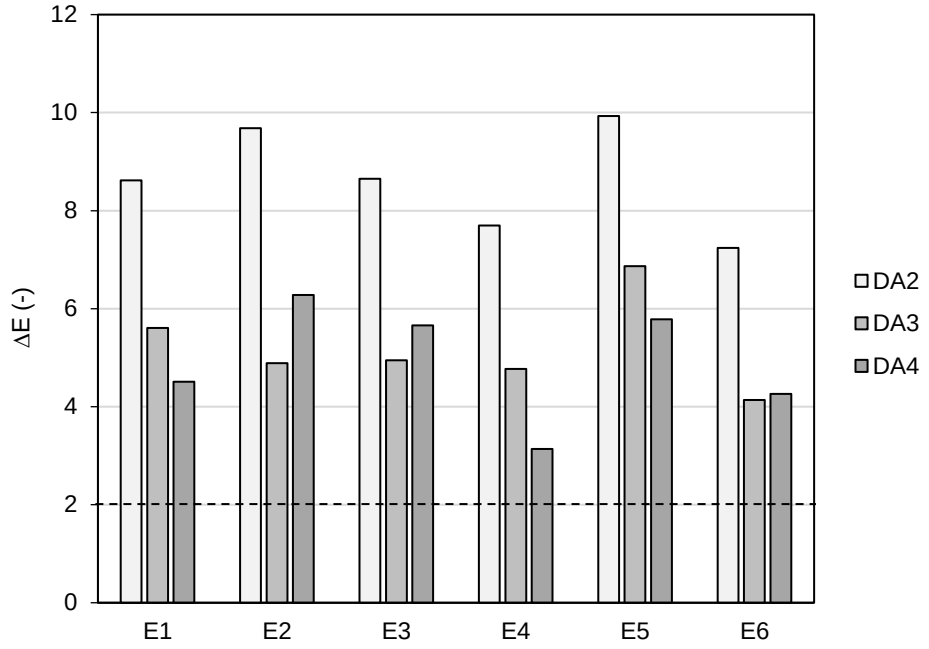

Figure 8. Average results of global colour variation on ETICS.

3.3. Static contact angle

The static contact angle of the systems with lower surface roughness (E1, E2, E5) are presented in Figure 9.

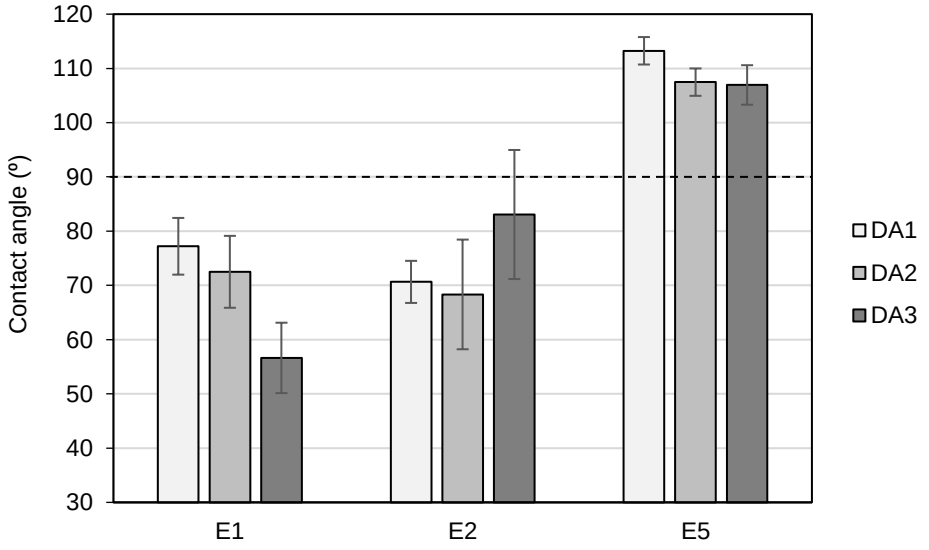

Figure 9. Static contact angle test results for E1, E2 and E5 systems (average values and relative standard deviation).

It can be observed that hygrothermal ageing leads to a slight decrease of the static contact angle (*i.e.*, higher wettability) for all tested systems. When comparing different systems, E5 (silicate-based FC) had hydrophobic

features (θ > 90º) also after hygrothermal and UV ageing tests, whereas E1 (acrylic-based FC) and E2 (lime-based rendering system) presented a hydrophilic surface (θ < 90º) [53].

System E1 underwent a significant θ decrease, especially after UV cycles (-27%). In agreement with the results reported by Quéré [46], higher values of surface roughness for hydrophilic surfaces lead to an even lower contact angle, as in the case of system E1 (Figure 5), if compared to the unaged system. System E2 also showed a slight θ decrease (higher wettability) after hygrothermal cycles, followed by a decrease of the wettability after the UV radiation accelerated test.

3.4. Optical microscopy and SEM-EDS analysis

When observing the surface of unaged and aged specimens by optical microscopy, a partial surface run-off was detected, especially after hygrothermal cycles for the systems with smoother surfaces (E2 and E5) (Figure 10 a,b). The formation of yellowish stains is noticed, as also confirmed through colorimetric analysis (Section 3.2). After the UV ageing test, a whitening of the surfaces can be generally observed (Figure 10 c,d), in accordance with previous observations (Section 3.2). Furthermore, some specimens gained a slightly darker tone after SO_2 weathering test (Figure 10 e,f).

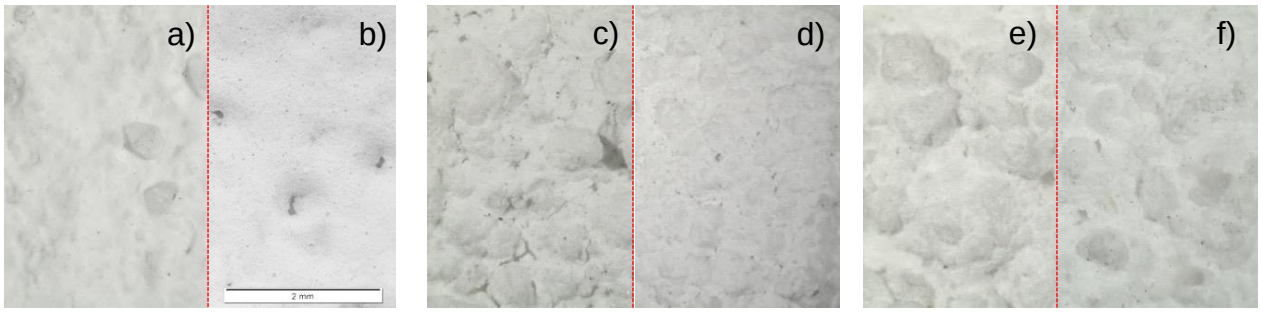

Figure 10. Microphotographs of system E2 a) unaged and b) after hygrothermal cycles; system E4 c) unaged and d) after UV cycles; and system E6 e) unaged and f) after SO_2 cycles.

Concerning SEM/EDS analyses, the systems finished with an acrylic-based FC (i.e., E1, E3, E6) show only a slight superficial run-off, which induced a more angular morphology on the particles, and some microcracks or micro lacunae, after both hygrothermal and UV cycles (Figure 11 a,b). A high percentage of Ca (attributed to the addition of calcium carbonate as pigment and filler) and of Ti (associated to the addition of TiO_2, which can be used both as pigment and photocatalytical additive) can be noticed in these systems (Figure 10 c). It is worth noting that additives with photocatalytical properties (*i.e.*, TiO_2 nanoparticles) are photo-activated by UV radiation and provide a self-cleaning capacity to the systems [54]. Thus, the addition of TiO_2 nanoparticles

can explain the low colour variation (higher light diffraction, closer to ideal white, as in the case of unaged specimens) observed after the UV ageing test (Section 3.2). The presence of oxide nanoparticles with photocatalytical activity reduce the transmittance of the UV radiations and prevent the photodegradation of the acrylic binder, in accordance with previous studies [55,56]. Furthermore, TiO_2 nanoparticles have also hydrophilic properties, and their addition can also explain the higher wettability of E1 after the UV ageing test (Section 3.3).

Conversely, the system finished with a hydraulic lime-based render (E2) was significantly affected by the hygrothermal cycles (Figure 11 d,e) and less significantly by UV radiation (Figure 11 f). In fact, calcium carbonate is highly hygroscopic and can undergo dissolution-reprecipitation processes, as well as more severe water leaching, if compared to systems with acrylic finishing. Furthermore, EDS elemental map confirmed the presence of high percentages of Ca (and no hint of Ti) (Figure 11 g).

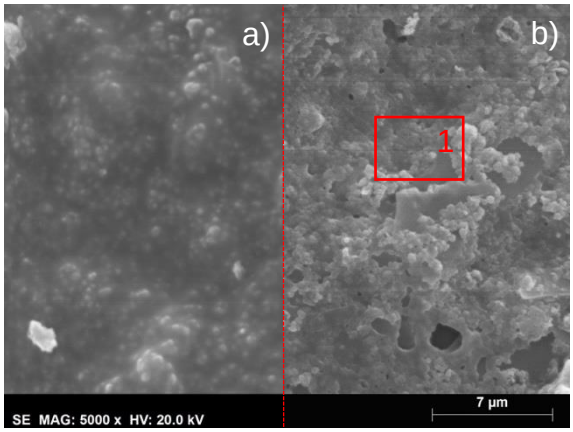

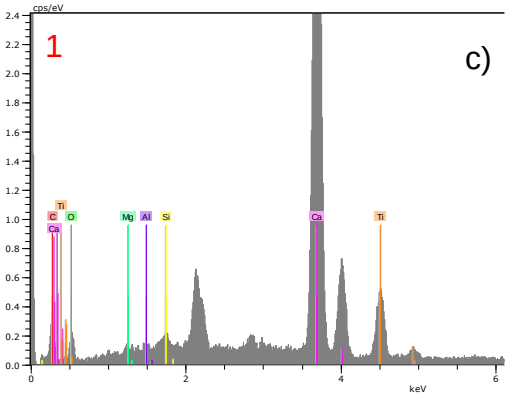

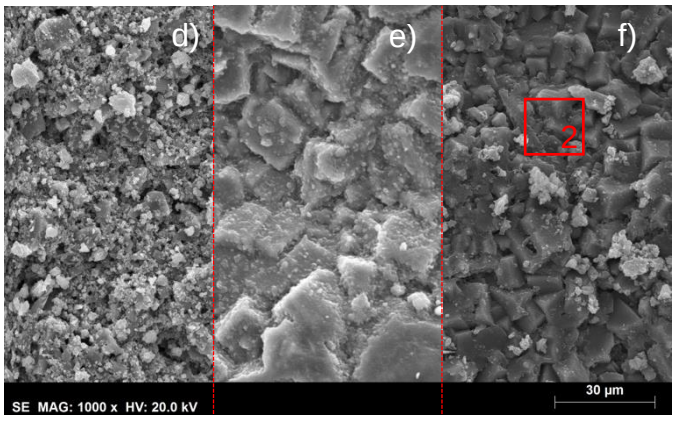

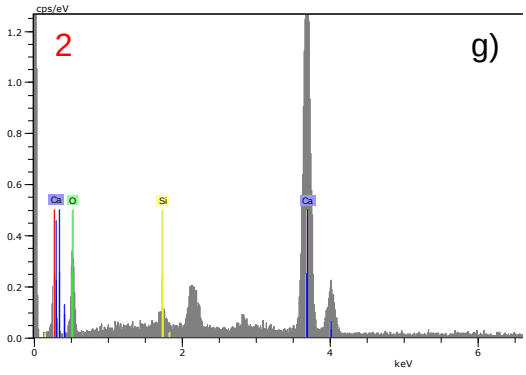

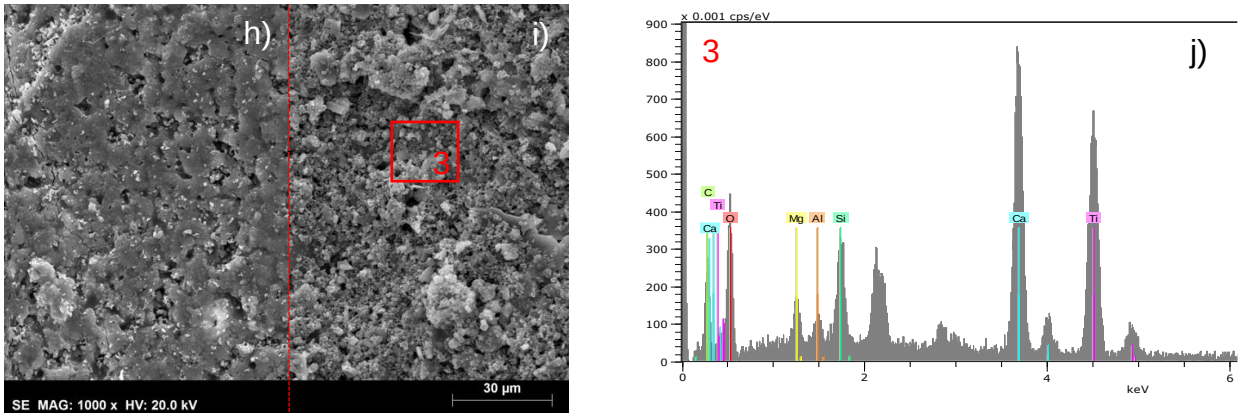

Figure 11. SEM microphotographs of system E1 a) unaged and b) after hygrothermal and UV cycles, and c) relative EDP elemental map; system E2 d) unaged and e) after hygrothermal and f) UV cycles, and g) relative EDP elemental map; system E5 h) unaged, i) after hygrothermal and UV cycles, and j) relative EDP elemental map.

System E5 presents a silicate-based FC, with superficial plate-like silica gel aggregate which forms a homogeneous patina [57]. The presence of calcium carbonate (present both in the hydraulic lime basecoat, and possibly also as pigment or filler in the coating) can favour the development of shorter linear chains of tetrahedral silica and linear silicate structure [58]. This superficial patina is also considerably affected after the hygrothermal and UV ageing tests, with particle cohesion loss and a more heterogeneous surface (Figure 11 h,i). It can be noticied that the amount of Si considerably decreased after the hygrothermal and UV ageing tests, whereas Ca and Ti amount increased (Figure. 11 l).

3.5. DRIFT analysis

The DRIFT spectra of all the systems after ageing by hygrothermal and UV cycles have no significant band shifting nor new bands that could be attributed to degradation products, when compared with the corresponding unaged sample spectra (Figure 12). The bands identified in all the spectra can be assigned to the ν*OH (broad band at ~ 3400 cm^{-1}), νCO_3^{2-} (centred at ~1450 cm^{-1}) and ωCO_3^{2-} out of the plane (at 876 cm^{-1}) modes. Other well-defined bands are observed, probably associated with the additives, such as ν*C=O (at 1874, 1795 and 1739 cm^{-1}) and ν_{as}Si-O-Si (1039 cm^{-1}) [51,59]. The band at ~1640 cm^{-1} is assigned to the δHOH mode of adsorbed water.

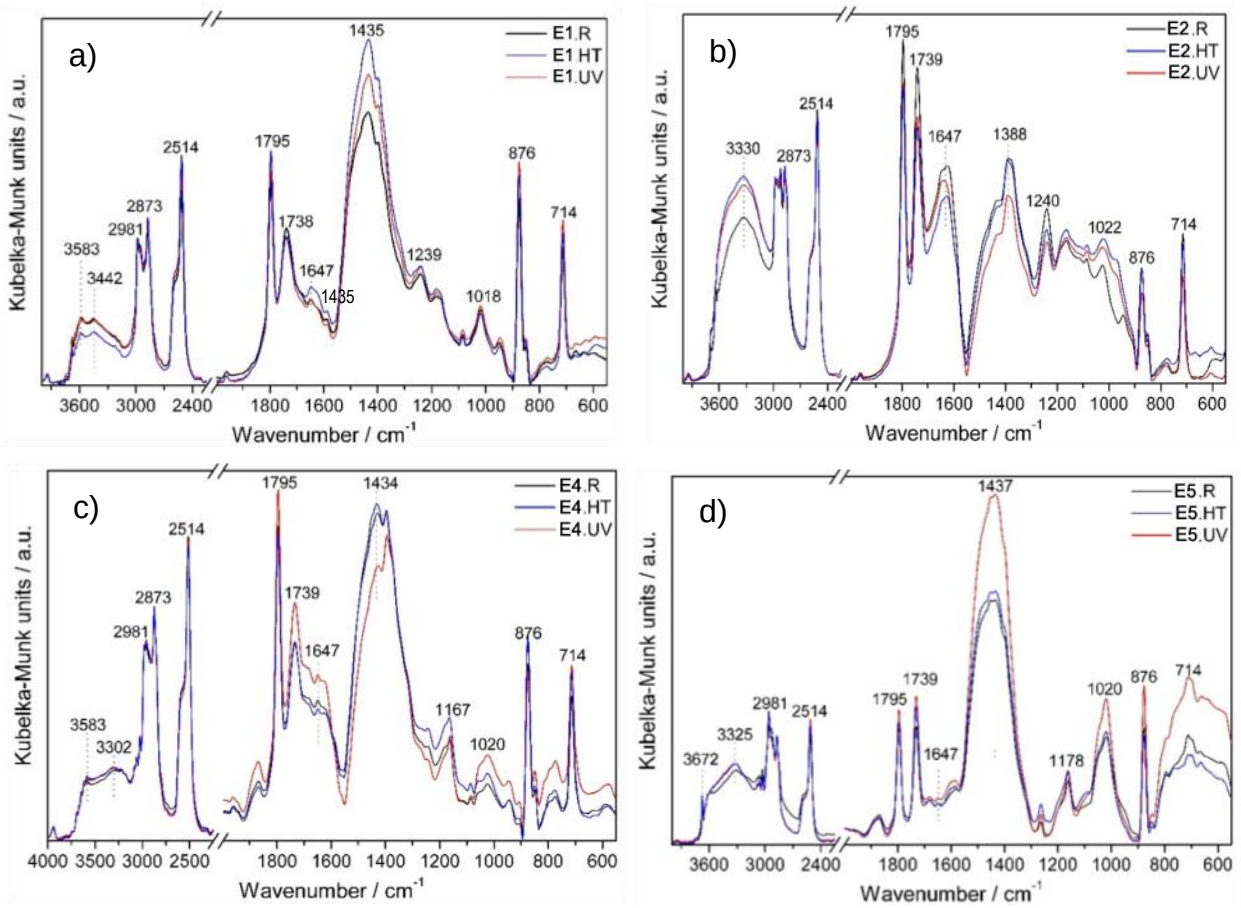

Figure 12. Regions of the DRIFT spectra of systems a) E1, b) E2, c) E4, d) E5, unaged (R) and after the hygrothermal (HT) and UV cycles (UV).

The DRIFT spectra showed that the more relevant effects of the ageing treatments consist in the alteration of the relative intensities of the carbonate (CO_3^{2-}) and hydroxyl (OH^-) bands, which can be associated to different carbonatation and hydrophilicity of the samples, respectively. Analysing the broad band centred at ~1430 cm^{-1} (overlapping of the $\nu_{as}CO_3^{2-}$, $\nu_sCO_3^{2-}$ and δCH_3 modes, Figure 12 a, b), and assuming that the changes are mainly due to carbonatation of the samples during the consecutive ageing cycles, it is worth noting a systematic increase of the carbonate relative amount in system E5. This may be associated to a migration of hydraulic lime of the basecoat to the silicate-based FC during ageing. Conversely, a systematic decrease of the carbonate relative amount is observed in the case of system E2, explainable by the probable degradation of the hydraulic lime in the FC (Figure 12, Table 5).

In the presence of acrylate polymers (e.g., E1, E4) and in case of their degradation, the yielded products can be acrylic monomers (with carbon-carbon double bonds), and so the assignment of the region near 1640 cm^{-1} becomes less straightforward, due to the νC=C band overlapping with the δHOH band of adsorbed water.

Additionally, the degradation of (methyl)acrylate films coincides with the relative intensity increase in the hydroxyl stretching region (3400 to 3200 cm^{-1}), which is caused by oxidation reactions [55]. The effect in the νOH band alongside the decrease and broadening of the carbonyl band at 1730 cm^{-1} and the appearance of a new carbonyl band at ~1780 cm^{-1}. In the DRIFT spectra of Figure 12 the OH band is significantly broad, due to a variety of OH interactions in the different systems, thus it is difficult to confirm the acrylate polymers degradation using this spectral region. Moreover, the changes observed in the carbonyl region cannot be directly related with polymeric coating degradation. To overcome this drawback and interpret the changes observed in the DRIFT spectra, a band deconvolution was performed to all the samples in two regions, namely 3740-2360 cm^{-1} and 1915-1100 cm^{-1}, as described in Section 2.3. The results are summarized in Table 5.

Table 5. Summary of the deconvolutions results by DRIFT for the ETICS systems.

Coating	Sample	HLB[(a)]	δHOH and νC=C[(b)]	CO_3^{2-} [(c)]
E1	R	1.28	0.20	0.57
	HT	0.88	0.28	0.61
	UV	1.19	0.22	0.51
E2	R	2.77	0.64	0.38
	HT	4.67	0.84	0.36
	UV	4.55	0.70	0.29
E3	R	0.79	0.26	0.44
	HT	0.81	0.27	0.41
	UV	0.97	0.34	0.46
E4	R	1.04	0.32	0.46
	HT	1.12	0.38	0.45
	UV	1.07	0.47	0.56
E5	R	2.29	0.34	0.68
	HT	2.71	0.45	0.68
	UV	3.17	0.47	0.74
E6	R	0.98	0.54	0.61
	HT	0.92	0.53	0.55
	UV	1.22	0.42	0.51

Notation: R – unaged specimens; HT – after hygrothermal cycles; UV – after UV cycles; [(a)] Hydrophilicity/lipophilicity balance: HLB = ΣAνOH/ΣAνCH; [(b)] Ratio: A(δHOH+νC=C)/ΣAνCH; [(c)] Relative carbonatation obtained by the ratio: $\Sigma A\nu CO_3^{2-}$/Area of 1915-1100 cm^{-1} region.

The values of HLB for coatings E2 and E5 are clearly higher than for the others, which is consistent with a system finished with a lime-based mortar (E2) or a silicate-based aqueous paint (E5).

If the coatings do not contain polyacrylates and/or if no degradation occurs during the ageing processes, the amount of adsorbed water correlates with the hydrophilicity of the samples, and thus the ratios A(δHOH)/ΣAνCH and ΣAνOH/ΣAνCH (HLB) should change concurrently. If partial degradation of the coatings occurs, some acrylate monomers will be left, with the $=CH_2$ deformation mode at ~1420 cm^{-1} overlapping with the carbonate bands, and the C=C stretch overlapping with the water deformation mode. In this case, the HLB and the A(δHOH)/ΣAνCH ratio are expected to behave differently. This happens for system E1, for which HLB decreases upon the first treatment, whereas the A(δHOH+AνC=C)/ΣAνCH increases. The process is reversed with the UV ageing process, suggesting a partial repair of the polymeric topcoat. This result may be explained by the presence of TiO_2 functionalised nanoparticles which can have a self-healing effect on coatings [60,61]. The sample E4.UV also presents a A(δHOH+AνC=C)/ΣAνCH ratio higher than expected comparing to the HLB, indicating that a slight degradation of the polyacrylates may have occurred. For sample E5.UV, which does not contain polyacrylates, the same ratio is lower than expected, suggesting a different decomposition by UV radiation, leading to OH groups, in accordance with results of Section 3.2.

It can be concluded that the acrylic coatings seem to present high degradation resistance after the hygrothermal and UV cycles, as also verified in Section 3.4.

3.6. Biological susceptibility to moulds

The results of the average rate of mould growth on the FC of the ETICS are shown in Table 6. The test was validated through the results obtained for the controls, all rated as 4 at the end of the test. The systems were already analysed in their sound state (DA1) and no growth was detected on the FC [12], due to the addition of biocide (Table 2). For the ageing cycles DA2 and DA4 and after 4 weeks of incubation, all systems were rated as 1 (traces of growth), which indicates a percentage of contaminated surface below 10% [35]. Moreover, following the criteria of standard NP 4505 [62], only one out of three tested replicates can be rated as 1 (traces of growth) in order to consider the paint of suitable quality and adequate performance for exterior applications. Therefore, all systems tested after the hygrothermal cycles, with exception of E4 and E5, fail to respect the criteria of NP 4505 [62].

Table 6. Average results of ETICS biological susceptibility to moulds.

System	DA2 (after hygrothermal cycles (HC))	DA4 (after HC + UV + SO_2)

	Week 1	Week 2	Week 3	Week 4	Week 1	Week 2	Week 3	Week 4
E1	0	0	0	0.66	0	0	0.66	0.66
E2	0	0.33	1	1	0	0	0.33	0.66
E3	0	0	0.33	0.66	0	0	0.33	0.33
E4	0	0	0.33	0.33	0	0	0	0.33
E5	0	0	0	0.33	0	0	0	0.33
E6	0	0.66	1	1	0	0	0.66	0.66
Control (paper)	3.33	4	4	4	3.33	3.67	4	4

Concerning the results after the complete ageing procedure (hygrothermal cycles + UV + SO_2), a slight decrease of mould growth was observed for systems E2, E3 and E6 when compared to DA2. This fact can find a possible justification in the presence of photocatalytic nanoparticles (TiO_2) on the FC formulation, as seen in previous sections. In fact, previous studies showed that the photocatalytical activity of TiO_2, activated by the UV light [63], can induce a high biocide effect, even at low concentration, with modification of the cell walls and of the cellular metabolism [64]. However, as mentioned above, all systems were rated as 1 either at DA2 or DA4, most probably due to the leaching of biocides during the ageing procedure [65] and no significant differences were found among test stages.

4. Discussion

The tests carried out in this study allowed to investigate the durability in simulated urban environments of six different commercially available ETICS. Results showed that no macroscopically visible cracking, loss of paint, detachments or surface irregularities were detected on the surface of the ETICS after the accelerated ageing cycles (*i.e.,* hygrothermal behaviour, UV and SO_2 ageing tests), although some surface run-off was observed mostly in the systems with smoother surfaces. Similar results were obtained in other studies, when evaluating different multilayer rendering systems, from ETICS [66,67] to thermal mortars [22] or other innovative construction systems [51].

The surface hardness of all systems slightly decreased after the complete ageing procedure (hygrothermal + UV + SO_2), being this effect more pronounced for the system finished with a lime-based rendering mortar (E2) and less pronounced for the system with a silicate-based finishing coat (E5). This decrease is indicative of some loss of cohesion of the FC [68]. As for surface roughness, results tended to be higher after the accelerated ageing procedure, although no clear pattern was defined among test stages. Nevertheless, the highest surface

roughness variation was again obtained for the system finished with a lime-based rendering mortar (E2) and the lowest for the silicate-based system (E5), which is in accordance with the results of surface hardness. In fact, a trend among surface hardness and surface roughness was found (Figure 13 a), regardless of the test stage, which is consistent with the referred relation between cohesion and surface hardness. The results show that the higher the surface roughness, the lower the surface hardness of the systems.

After a slight increase caused by the hygrothermal cycles, surface gloss decreased for all tested ETICS after the complete ageing procedure, possibly indicating a slight degradation of the coating [69]. The highest specular gloss decrease was obtained for the system with a co-polymeric resin FC (E6) and the lowest for the system finished with a lime-based mortar (E2). Figure 13b shows the correlations among surface gloss and surface roughness. The results suggest that the lower the roughness, the higher the gloss, in accordance with previous studies [12,70].

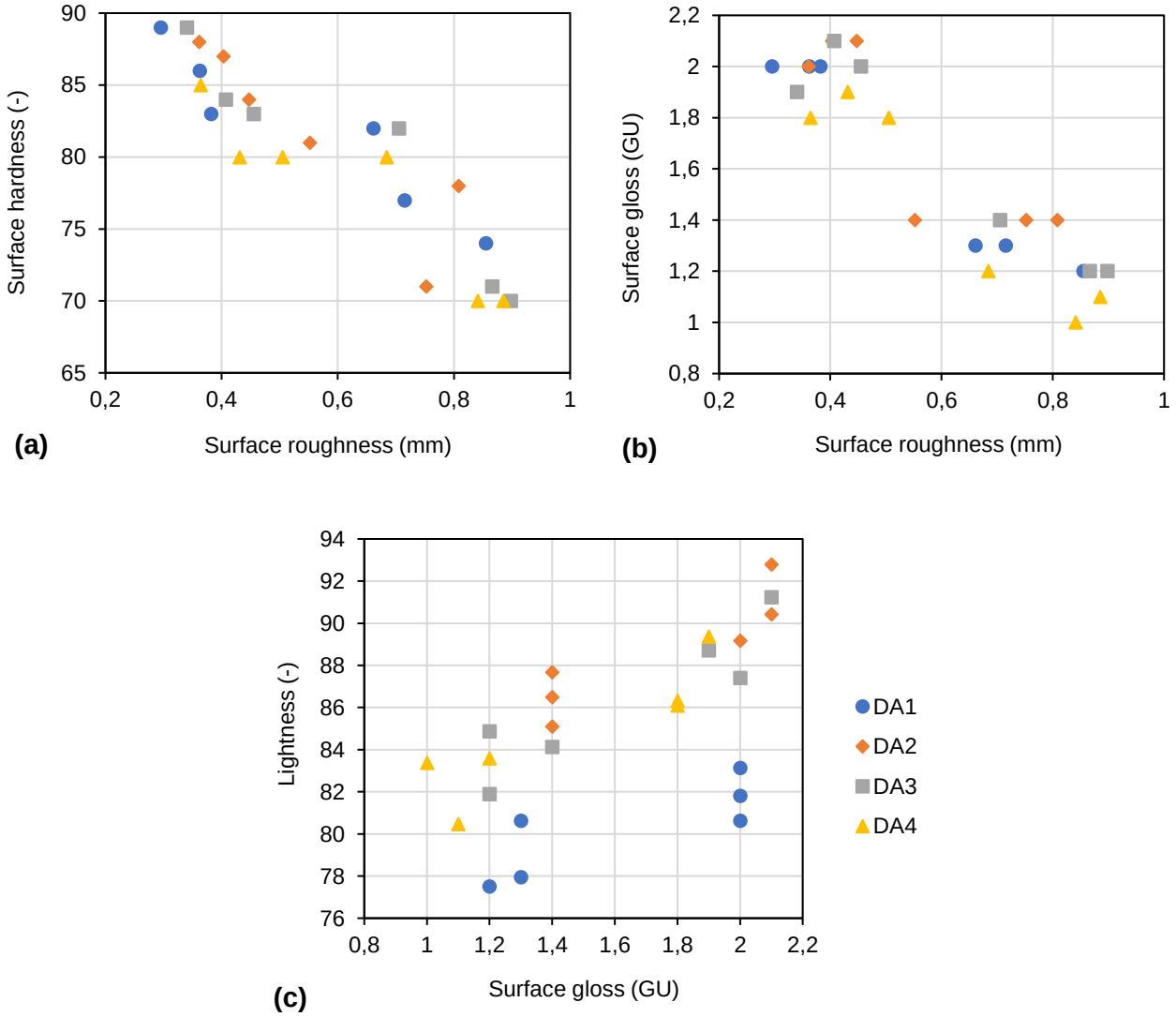

Figure 13. Correlations among surface hardness and surface roughness (a), surface gloss and surface roughness (b) and lightness and surface gloss (c) of all the ETICS throughout the ageing procedure.

Regarding the colour coordinates, a significant lightness (L*) increase was obtained after the hygrothermal cycles, and lower values were obtained after the UV and SO_2 ageing tests. Morphological observation (Section 3.4) confirmed that hygrothermal cycles affect the microstructure of the systems finishing coats, which can lead to L* variation. On the other hand, the systems showed high resistance to UV and SO_2 ageing tests, with even a whiter colour (if compared to the systems after hygrothermal cycles), which can be attributed to the self-healing properties of TiO_2 nanoparticles.

Additionally, lower values of surface roughness led to higher gloss (Figure 13b) and lightness (Figure 13c), by increasing light reflection [50,71].

The results confirmed substantial colour change for all systems ($\Delta E^*_{lab} > 2$, thus visible to the naked eye) after the hygrothermal cycles. After the complete ageing procedure, colour change results remained higher than 2 CIELAB units, in agreement with Paolini et al. [52].

Although no biological growth was detected for the sound ETICS, which can be explained by the presence of biocides [12], all systems subjected to hygrothermal cycles presented traces of growth after 4 weeks of incubation, possibly due to the leaching of biocides from the aged systems [65]. Moreover, no significant increase of mould growth was observed after UV and SO_2 ageing tests. In fact, slightly lower results were obtained for the ETICS finished with a lime-based mortar (E2), with an acrylic-based FC (E3), and for the system with a co-polymeric resin FC (E6). This trend can be possible explained by the presence of nanostructured TiO_2 on the finishing coat, which can have a biocide effect after UV light photoactivation [63].

The contact angle decreased for all tested systems (E1, E2, E5) after the hygrothermal cycles. Moreover, only the system with a silicate-based finishing coat (E5) has hydrophobic properties ($\theta > 90^o$) before and after ageing, whereas the systems with an acrylic-based finishing coat (E1) and finished with a lime-based rendering mortar (E2) have hydrophilic features ($\theta < 90^o$) on both unaged and aged conditions [53]. The results obtained for hydrophilic surfaces (E1 and E2) are in agreement with those obtained by Quéré [46], which observed an inverse correlation among surface roughness and the contact angle.

5. Conclusions

In this study, the durability of six different commercially available ETICS, when exposed to an innovative accelerated ageing procedure, which consists of hygrothermal, UV, and SO_2 ageing tests simulating urban environments, was assessed. The durability of the rendering system of the ETICS was evaluated by determining several physical and chemical-morphological properties prior and after each ageing cycle. The main conclusions of this study are the following:

- The surface hardness of the systems slightly decreased after the combined effect of the hygrothermal, UV and SO_2 ageing cycles, being this effect more pronounced for the system finished with a lime-based rendering mortar (E2). This latter system and the silicate-based finishing coat (E5) obtained the highest surface hardness results not only in the sound state, but also throughout the ageing procedure, when compared to the systems finished with an acrylic-based finishing coat. It can be concluded that systems finished with an acrylic coating and MW as thermal insulation (E4 and E6) have a significant hardness reduction after UV and/or SO_2 weathering tests.
- The results of surface roughness tended to be higher after the combined ageing procedure, although no clear pattern was defined among test stages. The surface roughness of the system with a silicate-based finishing coat (E5) was only slightly affected by the ageing procedure (+0.55%). Conversely, the surface roughness of the system finished with a lime-based rendering mortar (E2) significantly increased after the hygrothermal cycles (+36.6%), though no significant changes were observed after the UV or SO_2 exposure. The systems with an acrylic-based finishing coat (E3, E4 and E6) obtained the highest values of surface roughness both in their sound state and after the complete ageing procedure.
- After a slight increase caused by the hygrothermal cycles, surface gloss decreased for all systems after the combination of the selected ageing cycles. The highest specular gloss decrease was obtained for the system with a co-polymeric resin finishing coat (E6) and the lowest for the system finished with a lime-based mortar (E2). Substantial colour change was observed for all systems mainly after the hygrothermal cycles. After the combined ageing procedure, colour change results were lower than those after the hygrothermal cycles. Nevertheless, results remained higher than 2 CIELAB units, confirming an aesthetic alteration of the systems after ageing.

- Morphological and chemical analysis confirmed that acrylic and co-polymeric finishes (E1, E3, E4 and E6) exhibit low degradation. Furthermore, the addition of TiO_2 nanoparticles can provide improved biocide, self-cleaning and self-healing properties to the acrylic coating, especially after UV exposure.
- Traces of biological growth (< 10% of contaminated surface) were detected after the hygrothermal cycles mainly in the case of the systems finished with a lime-based rendering mortar (E2) and with a co-polymeric resin finishing coat (E6). No further increase of biocolonization was observed after UV and SO_2 exposure.
- Lower surface hydrophobicity was observed after the hygrothermal cycles for systems with lime-based (E2), acrylic-based (E1), and silicate-based (E5) rendering systems. The system with a silicate-based finishing coat maintained hydrophobic properties ($\theta > 90^{o}$) even after the artificial ageing, showing the best performance.

Future research intends to optimise the WGB_Shield accelerated ageing procedure through numerical simulation, considering the results obtained in the present study and southern European climatic conditions (using a representative Portuguese climate). Further tests are also ongoing with the aim of correlating natural and artificial ageing results, as well as quantifying the effects of biocide leaching and clarifying the possible synergistic effect induced by photocatalytical additives.

Acknowledgments

The authors acknowledge the support given by the Portuguese Foundation for Science and Technology (FCT) within the research project WGB_Shield (PTDC/ECI-EGC/30681/2017). J.L. Parracha acknowledges FCT for the Ph.D. scholarship (2020.05180.BD). The authors also acknowledge CIN, Saint-Gobain and Secil Martingança for the material supply, Dr. Pedro Nolasco from CQE/IST for the static contact angle tests and Marta Duarte from UPB/LNEC for the fungal tests.

References

[1] EU (2016) Mapping and analyses of the current and future (2020 – 2030) heating/cooling fuel deployment (fossil/renewables), European Commission.

[2] Energy Performance of Building Directive (EPBD) (2010). Directive 2010-31-EU of the European Parliament and of the Council, Official Journal of the European.

[3] A/RES/70/1 (2015) Transforming our world: the 2030 Agenda for Sustainable Development. United Nations.

[4] ECEEE (2018) Amending directive 2010/31/EU on the energy performance of buildings and Directive 2012/27/EU on energy efficiency. Official Journal of the European Union. European Commission

[5] Gonçalves, M., Simões, N., Serra, C., Flores-Colen, I., 2020. A review of the challenges posed by the use of vacuum panels in external insulation finishing systems. Applied Energy 257, 114028. https://doi.org/10.1016/j.apenergy.2019.114028

[6] Pasker, R., 2015. The European ETICS market - Facts & figures, in: European ETICS Forum 2015.

[7] Simona, P.L., Spiru, P., Ion, I. V., 2017. Increasing the energy efficiency of buildings by thermal insulation. Energy Procedia 128, 393–399. https://doi.org/10.1016/j.egypro.2017.09.044

[8] Varela Luján, S., Viñas Arrebola, C., Rodríguez Sánchez, A., Aguilera Benito, P., González Cortina, M., 2019. Experimental comparative study of the thermal performance of the façade of a building refurbished using ETICS, and quantification of improvements. Sustainable Cities and Society 51, 101713. https://doi.org/10.1016/j.scs.2019.101713

[9] Amaro, B., Saraiva, D., De Brito, J., Flores-Colen, I., 2013. Inspection and diagnosis system of ETICS on walls. Construction and Building Materials 47, 1257–1267. https://doi.org/10.1016/j.conbuildmat.2013.06.024

[10] García-Pérez, S., Sierra-Pérez, J., Boschmonart-Rives, J., 2018. Environmental assessment at the urban level combining LCA-GIS methodologies: A case study of energy retrofits in the Barcelona metropolitan area. Building and Environment 134, 191–204. https://doi.org/10.1016/j.buildenv.2018.01.041

[11] Silvestre, J.D., Castelo, A.M.P., Silva, J.J.B.C., Brito, J.M.C.L., Pinheiro, M.D., 2019. Retrofitting a building's envelope: Sustainability performance of ETICS with ICB or EPS. Applied Sciences 9. https://doi.org/10.3390/app9071285

[12] Parracha, J.L., Borsoi, G., Flores-Colen, I., Veiga, R., Nunes, L., Dionísio, A., Gomes, M.G., Faria, P., 2021. Performance parameters of ETICS: Correlating water resistance, bio-susceptibility and surface properties. Construction and Building Materials 272, 121956. https://doi.org/10.1016/j.conbuildmat.2020.121956

[13] Addleson, L., 1992. Building Failures: A guide to diagnosis, remedy and prevention. 3rd edition. Oxford, England. Butterworth Architecture.

[14] Malanho, S., Veiga, M. do R., 2020. Bond strength between layers of ETICS – Influence of the characteristics of mortars and insulation materials. Journal of Building Engineering 28. https://doi.org/10.1016/j.jobe.2019.101021

[15] Uygunoğlu, T., Özgüven, S., Çalış, M., 2016. Effect of plaster thickness on performance of external thermal insulation cladding systems (ETICS) in buildings. Construction and Building Materials 122, 496–504. https://doi.org/10.1016/j.conbuildmat.2016.06.128

[16] Sulakatko, V., Lill, I., Liisma, E., 2015. Analysis of On-site Construction Processes for Effective External Thermal Insulation Composite System (ETICS) Installation. Procedia Econ. Financ. 21, 297–305. https://doi.org/10.1016/s2212-5671(15)00180-x

[17] Steinbauer, V., Kaufmann, J., Zurbriggen, R., Bühler, T., Herwegh, M., 2017. Tracing hail stone impact on external thermal insulation composite systems (ETICS) – An evaluation of standard admission impact tests by means of high-speed-camera recordings. Int. J. Impact Eng. 109, 354–365. https://doi.org/10.1016/j.ijimpeng.2017.07.016

[18] Barreira, E., de Freitas, V.P., 2013. Experimental study of the hygrothermal behaviour of External Thermal Insulation Composite Systems (ETICS). Building and Environment 63, 31–39. https://doi.org/10.1016/j.buildenv.2013.02.001

[19] D'Orazio, M., Cursio, G., Graziani, L., Aquilanti, L., Osimani, A., Clementi, F., Yéprémian, C., Lariccia, V., Amoroso, S., 2014. Effects of water absorption and surface roughness on the bioreceptivity of ETICS compared to clay bricks. Building and Environment 77, 20–28. https://doi.org/10.1016/j.buildenv.2014.03.018

[20] Johansson, S., Wadsö, L., Sandin, K., 2010. Estimation of mould growth levels on rendered façades based on surface relative humidity and surface temperature measurements. Building and Environment 45, 1153–1160. https://doi.org/10.1016/j.buildenv.2009.10.022

[21] Daniotti, B. and Paolini, R. (2008) Experimental programme to assess ETICS cladding durability. In. 11 DBMC International Conference on Durability of Building Materials and Components. Istanbul, Turkey, 11-14 May 2008.

[22] Maia, J., Ramos, N.M.M., Veiga, R., 2019. Assessment of test methods for the durability of thermal

mortars exposure to freezing. Materials and Structures 52, 1–14. https://doi.org/10.1617/s11527-019-1411-4

[23] Esteves, C., Ahmed, H., Flores-Colen, I., Veiga, R. The influence of hydrophobic protection on building exterior claddings. Journal of Coatings Technology and Research 16, 1379-1388. https://doi.org/10.1007/s11998-019-00220-7

[24] Roncon, R., Borsoi, G., Parracha, J.L., Flores-Colen, I., Veiga, R., Nunes, L. Impact of water-repellent products on the moisture transport properties and mould susceptibility of External Thermal Insulation Composite Systems. Article submitted to Coatings.

[25] EOTA (European Organisation for Technical Approvals), 2020. EAD 040083-00-0404: External thermal insulation composite systems (ETICS) with rendering. Guidel. Eur. Tech. Approv. 1–88.

[26] NT BUILD 495 (2000) Nordtest method. Building materials and components in the vertical position: exposure to accelerated climatic strains. Nordic Council of Ministers, Finland.

[27] Griciutė, G., Bliūdžius, R., Norvaišienė, R., 2013. The Durability Test Method for External Thermal Insulation Composite System used in Cold and Wet Climate Countries. J. Sustain. Archit. Civ. Eng. 1, 50–56. https://doi.org/10.5755/j01.sace.1.2.2778

[28] Bochen, J., Gil, S., 2009. Properties of pore structure of thin-layer external plasters under ageing in simulated environment. Construction and Building Materials 23, 2958–2963. https://doi.org/10.1016/j.conbuildmat.2009.02.041

[29] Slusarek, J., Orlik-Kozdón, B., Bochen, J., Muzyczuk, T., 2020. Impact of the imperfection of thermal insulation on structural changes of thin-layer façade claddings in ETICS. Journal of Building Engineering 32, 101487. https://doi.org/10.1016/j.jobe.2020.101487

[30] Lewry, A.J., Crewdson, L.F.E., 1994. Approaches to testing the durability of materials used in the construction and maintenance of buildings. Construction and Building Materials 8, 211-222. https://doi.org/10.1016/S0950-0618(09)90004-6

[31] Kvande, T., Bakken, N., Bergheim, E., Thue, J.V., 2018. Durability of ETICS with rendering in Norway-Experimental and field investigations. Buildings 8. https://doi.org/10.3390/buildings8070093

[32] ISO 16474-3 (2013) Paints and varnishes – Methods of exposure to laboratory light sources – Part 3: Fluorescent UV lamps. Geneva, Switzerland.

[33] Gomes, V., Dionísio, A., Pozo-Antonio, J.S., 2018. The influence of the SO_2 ageing on the graffiti

cleaning effectiveness with chemical procedures on a granite substrate, Science of the Total Environment 625, 233–245. https://doi.org/10.1016/j.scitotenv.2017.12.291

[34] E. E. Agency (2017) Sulfur dioxide (SO_2): Annual mean concentrations in Europe. http://www.eea.europa.eu/themes/air/interactive/so2

[35] ASTM D5590-17 (2017) Determining the resistance of paint films and related coatings to fungal defacement by accelerated four-week agar plate assay. ASTM International, Pennsylvania, USA.

[36] ASTM C1338-19 (2019) Standard test method for determining fungi resistance of insulation materials and facings. ASTM International, Pennsylvania, USA.

[37] ASTM D2240 (2000) Standard test method for rubber property – durometer hardness. ASTM International, West Conshohocken, PA, USA.

[38] CIE S014-4/E (2007) Colorimetry part 4: CIE 1976 L*a*b* colour space. Commission Internationale de l'eclairage. CIE Central Bureau, Vienna, Austria.

[39] Mokrzycki, W. and Tatol, M. (2011) Color difference Delta E-A survey. Machine Graphics and Vision 20, 383-411.

[40] EN 15802 (2009) Conservation of cultural property. Test methods. Determination of static contact angle. European Committee for Standardization, Brussels, Belgium.

[41] Fidelio, A., Ciriminna, R., Ilharco, L.M., Pagliaro, M. (2005) Role of the Alkyl-Alkoxide Precursor on the Structure and Catalytic Properties of Hybrid Sol-Gel Catalysts, Chem. Mater. 17, 26, 6686–6694. https://doi.org/10.1021/cm051954x

[42] Galvão, J., Flores-Colen, I., de Brito, J., Veiga, M.R., 2018. Variability of in-situ testing on rendered walls in natural ageing conditions – Rebound hammer and ultrasound techniques. Construction and Building Materials 170, 167–181. https://doi.org/10.1016/j.conbuildmat.2018.02.152

[43] Mirabedini, S.M., Sabzi, M., Zohuriaan-Mehr, J., Atai, M., Behzadnasab, M., 2011. Weathering performance of the polyurethane nanocomposite coatings containing silane treated TiO 2 nanoparticles. Applied Surface Science 257, 4196–4203. https://doi.org/10.1016/j.apsusc.2010.12.020

[44] Momber, A.W., Irmer, M., Glück, N., 2017. Effects of accelerated low-temperature ageing on the performance of polymeric coating systems on offshore steel structures. Cold Reg. Sci. Technol. 140, 39–53. https://doi.org/10.1016/j.coldregions.2017.04.005

[45] Rashvand, M., Ranjbar, Z., 2014. Degradation and stabilization of an aromatic polyurethane coating

during an artificial aging test via FTIR spectroscopy. Mater. Corros. 65, 76–81. https://doi.org/10.1002/maco.201206544

[46] Quéré, D. (2005) Non-sticking drops. Reports on Progress in Physics 68, 2495-2532. https://doi.org/10.1088/0034-4885/68/11/R01

[47] García, O., Malaga, K., 2012. Definition of the procedure to determine the suitability and durability of an anti-graffiti product for application on cultural heritage porous materials. Journal of Cultural Heritage 13, 77–82. https://doi.org/10.1016/j.culher.2011.07.004

[48] Saha, S., Kocaefe, D., Boluk, Y., Pichette, A., 2011. Enhancing exterior durability of jack pine by photo-stabilization of acrylic polyurethane coating using bark extract. Part 1: Effect of UV on color change and ATR-FT-IR analysis. Progress in Organic Coatings 70, 376–382. https://doi.org/10.1016/j.porgcoat.2010.09.034

[49] Shirakawa, M.A., de Lima, L.N., Gaylarde, C.C., Silva Junior, J.A., Loz, P.H.F., John, V.M., 2020. Effects of natural aging on the properties of a cool surface exposed in different Brazilian environments. Energy and Buildings 221. https://doi.org/10.1016/j.enbuild.2020.110031

[50] Xie, T., Kao, W., Sun, L., Wang, J., Dai, G., Li, Z., 2020. Preparation and characterization of self-matting waterborne polymer–An overview. Progress in Organic Coatings 142, 105569. https://doi.org/10.1016/j.porgcoat.2020.105569

[51] D'Orazio, M., Stipa, P., Sabbatini, S., Maracchini, G., 2020. Experimental investigation on the durability of a novel lightweight prefabricated reinforced-EPS based construction system. Construction and Building Materials 252, 119134. https://doi.org/10.1016/j.conbuildmat.2020.119134

[52] Paolini, R., Zani, A., Poli, T., Antretter, F., Zinzi, M., 2017. Natural aging of cool walls: Impact on solar reflectance, sensitivity to thermal shocks and building energy needs. Energy and Buildings 153, 287–296. https://doi.org/10.1016/j.enbuild.2017.08.017

[53] Ploeger, R., Musso, S., Chiantore, O., 2009. Contact angle measurements to determine the rate of surface oxidation of artists' alkyd paints during accelerated photo-ageing. Progress in Organic Coatings 65, 77–83. https://doi.org/10.1016/j.porgcoat.2008.09.018

[54] Liu, G., Xia, H., Niu, Y., Zhao, X., Zhang, G., Song, L., Chen, H., 2021. Fabrication of self-cleaning photocatalytic durable building coating based on WO3-TNs/PDMS and NO degradation performance. Chem. Eng. J. 409, 128187. https://doi.org/10.1016/j.cej.2020.128187

[55] Aguirre, M., Goikoetxe, M., Otero, L.A., Paulis, M., Leiza, J.R. (2017) Accelerated ageing of hybrid acrylic waterborne coatings containing metal oxide nanoparticles: Effect on the microstructure. Surface and Coatings Technology, 321, 484-490. https://doi.org/10.1016/j.surfcoat.2017.05.013

[56] Fjellstrom, H., Hoglund, H., Forsberg, S., Paulsson, M. (2009) The UV-screening properties of coating layers: the influence of pigments, binders and additives. Nordic Pulp and Paper Research Journal, 24, 206-212. https://doi.org/10.3183/NPPRJ-2009-24-02-p206-212

[57] Borsoi, G., Tavares, M., Veiga, R., Santos Silva, A. (2012) Microstructural Characterization of Consolidant Products for Historical Renders: An Innovative Nanostructured Lime Dispersion and a More Traditional Ethyl Silicate Limewater Solution, Microstructure and Microanalysis 18, 1181–1189. https://doi.org/10.1017/S1431927612001341

[58] Zendri, E., Biscontin, G., Nardini, I., Rialto, S. (2007) Characterization and reactivity of silicatic consolidants, Construction and Building Materials 21, 1098–1106. https://doi.org/10.1016/j.conbuildmat.2006.01.006

[59] Júlio, M.F., Soares, A., Ilharco, L.M., Flores-Colen, I., de Brito, J., Silica-based aerogels as aggregates for cement-based thermal renders, Cement and Concrete Composites 72, 309-318. https://doi.org/10.1016/j.cemconcomp.2016.06.013

[60] Vijayan, P., Al-Maadeed, M.A., TiO_2 nanotubes and mesoporous silica as containers in self-healing epoxy coatings. Scientific Reports 6, 38812. https://doi.org/10.1038/srep38812

[61] Ghomi, E.R., Khorasani, S.N., Kichi, M.K., Dinari, M., Ataei, S., Enayati, M.H., Koochaki, M.S., Neisiany, R.E. (2020) Synthesis and characterization of TiO_2/acrylic acid-co-2-acrylamido-2-methyl propane sulfonic acid nanogel composite and investigation its self-healing performance in the epoxy coatings, Colloid and Polymer Science, 298, 213–223. https://doi.org/10.1007/s00396-019-04597-0

[62] NP 4505 (2012) Paints and varnishes. Paints for exterior surfaces of buildings. Classification and requirements. Norma Portuguesa, Instituto Português da Qualidade, Caparica, Portugal (in Portuguese).

[63] Gaylarde, C.C., Morton, L.H.G., Loh, K., Shirakawa, M.A., 2011. Biodeterioration of external architectural paint films - A review. International Biodeteriorioration & Biodegradation 65, 1189–1198. https://doi.org/10.1016/j.ibiod.2011.09.005

[64] Kubacka, A., Suarez-Diez, M., Rojo, D., Bargiela, R., Ciordia, S., Zapico, i., Albar, J.P., Barbas, C., Martins dos Santos, V.A.P., Fernández-García, M., Ferrer, M., Understanding the antimicrobial

mechanism of TiO2-based nanocomposite films in a pathogenic bacterium, Scientific Reports 4(1):4134. https://doi.org/10.1038/srep04134

[65] Vega-Garcia, P., Schwerd, R., Scherer, C., Schwitalla, C., Johann, S., Rommel, S.H., Helmreich, B., 2020. Influence of façade orientation on the leaching of biocides from building façades covered with mortars and plasters. Science of the Total Environment 734, 139465. https://doi.org/10.1016/j.scitotenv.2020.139465

[66] Griciutė, G., Bliūdžius, R., 2015. Study on the microstructure and water absorption rate changes of exterior thin-layer polymer renders during natural and artificial ageing. Medziagotyra 21, 149–154. https://doi.org/10.5755/j01.ms.21.1.4869

[67] Norvaišiene, R., Griciute, G., Bliudžius, R., Ramanauskas, J., 2013. The changes of moisture absorption properties during the service life of external thermal insulation composite system. Medziagotyra 19, 103–107. https://doi.org/10.5755/j01.ms.19.1.3834

[68] Girginova, P.I., Galacho, C., Veiga, R., Santos Silva, A., Candeias, A., 2020, Study of mechanical properties of alkaline earth hydroxide nanoconsolidants for lime mortars, Construction and Building Materials 236, 117520. https://doi.org/conbuildmat.2019.117520

[69] Tilley, R. (2000) Colour and the Optical Properties of Materials, Wiley, Chichester, England.

[70] Ochs, H., Vogelsang, J., Meyer, G., 2003. Enhanced surface roughness of organic coatings due to UV-degradation: An unknown source of EIS-artifacts. Progress in Organic Coatings 46, 182–190. https://doi.org/10.1016/S0300-9440(03)00004-3

[71] Faucheu, J., Wood, K.A., Sung, L.P., Martin, J.W., 2006. Relating gloss loss to topographical features of a PVDF coating. Journal of Coatings Technology and Research 3, 29–39. https://doi.org/10.1007/s11998-006-0003-8